

## NATURAL CONVECTION IN A VENTILATED DOUBLE GLASS WINDOW

**Taynara Geysa Silva do Lago**

**Kamal Abdel Radi Ismail**

**Mário Ventura Mondlane**

*taynaragsl@fem.unicamp.br*

*kamal@fem.unicamp.br*

*mondlane1988@fem.unicamp.br*

*State University of Campinas (UNICAMP)*

*Faculty of Mechanical Engineering, Department of Energy, 13083-860, Campinas, São Paulo, Brazil*

**Abstract.** This study presents the numerical results of the flow problem induced by natural convection in a channel between asymmetrically heated vertical parallel glass sheets of a ventilated double glass window. The model is based on the equations of conservation of mass, energy and momentum in its two-dimensional forms. The Finite Volume Method was used in the resolution with discretization schemes of central differences for diffusive terms and Power Law for the convective terms. For the coupling of pressure and velocity the SIMPLE algorithm is used, while the TDMA method is used in the solution of the systems of equations. The numerical code is used to determine the velocity and temperature fields between the glass sheets under real ambient conditions and asymmetric heating conditions. The results were validated with available literature results indicating that the model is adequate to solve this type of problem.

**Keywords:** Natural convection, Double glass, Passive comfort.

## **1 Introduction**

The thermal performance and energy efficiency of a building are themes that have renewed the interest of their investigation in today's society. With regard to human thermal comfort, it is extremely important for the high performance of human beings in their daily life and the execution of their activities until rest (day and night). Thermal performance and energy efficiency are concepts associated with thermal comfort, which refers to the mental state that expresses man's satisfaction with the surrounding thermal environment.

Most buildings (especially commercial types) usually have external envelopes with large glazed areas where solar radiation heat can penetrate (or escape) causing undesirable heat gain (or loss) inside the buildings provoking increase of the energy consumption. To reduce this energy consumption (winter heating and summer cooling) and consequent reduction of CO<sub>2</sub> emissions to the atmosphere, windows of different concepts were investigated among which ventilated double glass windows have emerged as an alternative to improve indoor comfort conditions and enhance energy efficiency of buildings.

The flow of a fluid between the two glass sheets of a window has been pointed out as an efficient solution for cold and hot climates. This type of windows is known as ventilated window, composed of double or triple glass sheets with open ends and an air flow duct formed by the glass sheets. Several studies on this type of ventilated window can be found in the literature.

The use of movable shutter installed between the glass plates for the double-glazed window system reached an energy saving of about 36% during the winter, and 47% during the summer by using this type of window in typical Canadian weather conditions [1]. Zhang et al. [2] investigated numerically an insulated shutter installed inside a cavity formed by two glass sheets. The authors focused their analysis on the effect of the shutter on the temperature distribution, the flow field due to natural convection in the cavity and on the global coefficient of heat transfer.

The ventilated window can be used continuously to satisfy the required ventilation of the space with a small penalty on the cooling load during the summer [3]. A new ventilated window incorporating a rotating frame with two glass sheets, in summer, absorbs the incident solar radiation through the absorbent glass facing the outside environment and heats the air which is expelled outwards. In winter, the window is rotated so that the absorbent surface is in contact with the internal environment reducing heat losses and allowing heated air to enter the building [4]. The effect of determining the ideal width of a double glass channel and the temperature of the cold wall allows establishing flux value in the closed double glass channel. The effects of the external convective coefficient have no significant effect on the heat transfer towards the internal space [5, 6].

Ismail and Henriquez [7, 8, 9] developed three studies on two-dimensional transient numerical model for the heat transfer through a simple glass window, double glass and double glass ventilated window with forced airflow, respectively. The authors concluded that for a clear glass and different thicknesses, the solar heat gain coefficient remains almost constant, and that the spacing between the glass sheets has little effect on the Solar Heat Gain Coefficient, SHGC, and on the Shading Coefficient. Besides, that the effect of the increase of the mass flow rate over the thermal behavior of the ventilated glass window is to decrease the mean Solar Heat Gain Coefficient and the Shading Coefficient and that the radiative exchange effect has no significant influence.

The use of absorbing gases between glass sheets in the double glass ventilated window is an alternative solution for thermally insulated glass windows. Other options one can incorporate filling materials such as silica aerogel or a PCM. The glass sheets filled with PCM or an absorbent gas are more effective than single glass and double glass window as reported in [10, 11].

Window of single-and dual-channel airflow, including a reversible window frame was presented in [12, 13]. These window systems are not suitable for subtropical or tropical climates and that during summer significant energy consumption can be required. Chow et al. [14] introduced a water-flow window. Three cases were studied in order to reduce air conditioning load and enhancing thermal and visual comfort and concluded that the combination of tinted glass-water-clear glass is the best energy saving arrangement.

Recently, a precise study based upon the spectral effects on the transmittance and solar heat gain was applied to analyze a glazing layer [15]. The bulk properties spectral quantities ( $\tau$ ,  $\rho$  and  $\alpha$ ) were

calculated using software Window. Energy-10 [16, 17] also software was developed to be used for the calculation of thermal parameters in studies related with solar control films in single and multiple glass window units.

In the present study, the thermal behavior of a ventilated double glass arrangement is numerically investigated. The model is based on the conservation equations of mass, momentum and the energy. The discretization of conservative equations is done by using the finite volume method. The model is validated against available results and then used to calculate the temperature and flow fields as well as the solar heat gain coefficient.

## 2 Mathematic of model

The double glass window system is an efficient arrangement for windows where the air flows in the gap between the glass sheets absorbing the solar radiation, reducing penetrated heat to the internal ambient and providing natural ventilation as shown in Fig. 1. A model for the double glass window is made by following the incident rays that propagate through the system, incident solar radiation is shown on the left hand side, in the second region heat is exchanged by convection between the outer surface and the external environment while in the third region heat flux is exchanged by radiation with the internal environment.

Figure 1 shows the physical model of the problem to be studied where air flow is induced by natural convection in a channel formed by two parallel glass sheets with non-symmetric heating. The air flow is induced up into the channel by the buoyancy forces due to the thermal effects. When the solar energy strikes the external glass, part of it is reflected, part is absorbed and another part is transmitted. The energy passing through the external glass ( $I_{o1}$ ) is directed to the internal glass, part of this energy is reflected while another part is absorbed and transmitted to internal environment.

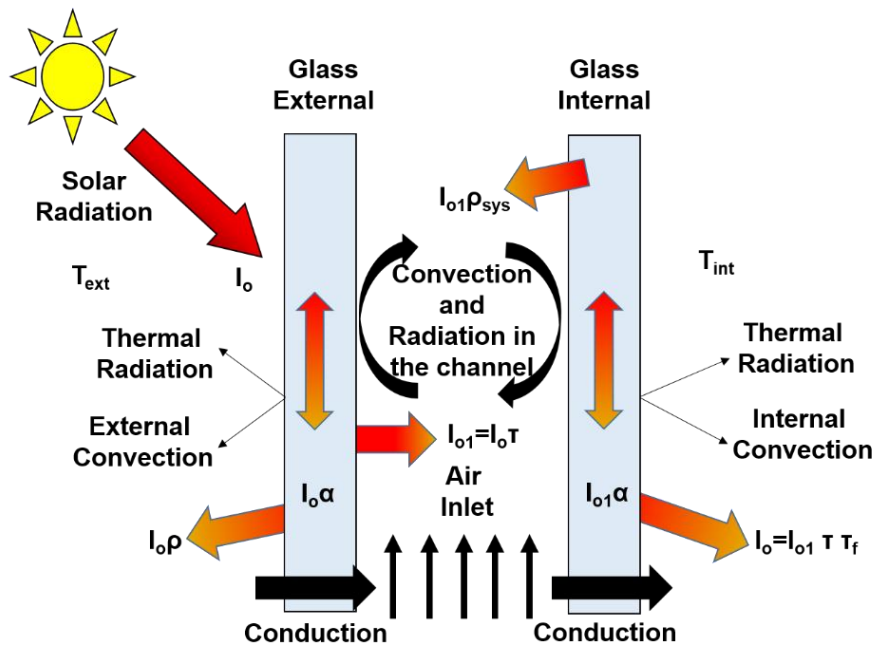


Figure 1. The physical model of the ventilated double glass window.

The computational domain of the model is represented by the double glass sheets of height ( $H$ ), and a gap of width ( $b$ ) between the glass sheets as shown in Fig. 2. Glass 1 facing the external environment at temperature ( $T_{ext}$ ) is exposed to solar radiation ( $I_o$ ), and glass 2 facing the room with an inside temperature ( $T_{int}$ ). The external surface of the external glass sheet is subjected to convection and radiation ( $q_{conv-ext}$ ) and ( $q_{rad-ext}$ ) while the inner surface of the internal glass sheet exchanges heat with



## 2.2 Conservation equations for glass sheets

The velocity components  $u$  and  $v$  are zero on the glass surface. As a result of the energy balance on the glass region, the differential equation for the temperature distribution over the wall domain is:

$$\frac{k_g}{\rho_g c p_g} \left( \frac{\partial^2 T}{\partial x^2} + \frac{\partial^2 T}{\partial y^2} \right) - \frac{1}{\rho_g c p_g} \frac{\partial I}{\partial x} = 0 \quad (5)$$

The term  $\partial I / \partial x = I_0 \exp[\kappa(t-x)]$ , in Eq. (5), where  $\kappa$  is the glass extinction coefficient and  $t$  is the glass thickness, Siegel [18]. This term will be used to compute the solar radiation absorbed by the glass sheets since this region is semitransparent to solar radiation. On the other hand, in the region of channel, the air does not absorb solar radiation and therefore the source term in the energy equation will be null when the equation is applied to the fluid region.

## 2.3 Boundary conditions for the channel

Figure 2 shows the general layout of the problem and the associated boundary conditions. In the channel region  $u=v=0$ , there is no slip velocity on the glass surfaces. The air enters the channel at temperature  $T_{int}$  while the temperature gradient in vertical direction at exit is null. These conditions are:

Channel entry,

$$\frac{\partial u}{\partial y} = \frac{\partial v}{\partial y} = 0, T = T_{int} \text{ for } x_1 < x < x_2 \text{ and } y=0 \quad (6)$$

Channel exit,

$$\frac{\partial u}{\partial y} = \frac{\partial v}{\partial y} = \frac{\partial T}{\partial y} = 0 \text{ for } x_1 < x < x_2 \text{ and } y=H \quad (7)$$

Internal surfaces of the channel,

$$q_{conv-1} + q_{rad-1} + k_{g1} \frac{\partial T_{g1}}{\partial x} = 0 \text{ for } x=x_1 \text{ and } 0 \leq y \leq H \quad (8)$$

$$q_{conv-2} + q_{rad-2} + k_{g2} \frac{\partial T_{g2}}{\partial x} = 0 \text{ for } x=x_2 \text{ and } 0 \leq y \leq H \quad (9)$$

## 2.4 Boundary conditions on the glass sheets

For glass 1, at  $x=0$  the vertical boundary exchanges heat by radiation and convection with the external air ( $T_{ext}=32^\circ\text{C}$ ). At  $x=x_1$  conduction occurs on the glass sheet and convection towards the enclosed air between the sheets. Glass-2 exchanges heat by convection and radiation with the internal environment (room) at  $T_{int}=24^\circ\text{C}$ . The horizontal boundaries are kept thermally insulated. Hence the energy balance can be written as:

Glass 1,

$$-k_g \frac{\partial T_{g1}}{\partial y} = h_{ext} [T_{g1} - T_{ext}] + \sigma \varepsilon_g [T_{g1}^4 - T_{ext}^4] \text{ for } x=0 \text{ and } 0 \leq y \leq H \quad (10)$$

$$-k_g \frac{\partial T_{g1}}{\partial y} = q_{conv-1} + q_{rad-1} \text{ for } x=x_1 \text{ and } 0 \leq y \leq H \quad (11)$$

$$\frac{\partial T_{g1}}{\partial y} = 0 \text{ for } 0 < x < x_1 \text{ and } y=0 \quad (12)$$

$$\frac{\partial T_{g1}}{\partial y} = 0 \text{ for } 0 < x < x_1 \text{ and } y=H \quad (13)$$

Glass 2,

$$-k_g \frac{\partial T_{g2}}{\partial y} = h_{\text{int}} [T_{g1} - T_{\text{int}}] + \sigma \varepsilon_g [T_{g2}^4 - T_{\text{int}}^4] \text{ for } x=x_3 \text{ and } 0 \leq y \leq H \quad (14)$$

$$-k_g \frac{\partial T_{g2}}{\partial y} = q_{\text{conv}-2} + q_{\text{rad}-2} \text{ for } x=x_2 \text{ and } 0 \leq y \leq H \quad (15)$$

$$\frac{\partial T_{g2}}{\partial y} = 0 \text{ for } x_2 < x < x_3 \text{ and } y=0 \quad (16)$$

$$\frac{\partial T_{g2}}{\partial y} = 0 \text{ for } x_2 < x < x_3 \text{ and } y=H \quad (17)$$

## 2.5 Evaluation of SHGC

The quantity that allows the thermal evaluation of the double glass window is the total heat flux ( $q_{\text{total-int}}$ ), which passes through the double glazing and reaches the internal ambient. The components of the total heat flux are: convective flux ( $q_{\text{conv-int}}$ ), radiative flux ( $q_{\text{rad-int}}$ ), and the energy transmitted directly ( $q_{\text{total-int}}=I_{o2}$ ).

According to Fig. 2, one can write:

$$q_{\text{total-int}} = q_{\text{conv-int}} + q_{\text{rad-int}} + I_{o2} \quad (18)$$

According to Fig. 2, one can write The Solar Heat Gain Coefficient (SHGC) is a useful parameter to indicate the efficiency of a system formed by one or several glass sheets. To calculate the SHGC, Eq. (18) is divided by the incident solar radiation  $I_o$ , to obtain:

$$\text{SHGC} = \frac{q_{\text{conv-int}} + q_{\text{rad-int}} + I_{o2}}{I_o} \quad (19)$$

## 3 Numerical treatment

The FORTRAN home-built simulation code has been developed based on the finite volume technique to solve the governing differential equations and the associated boundary conditions. The Power-law scheme is used for discretizing the convective and diffusive energy fluxes. The computational code uses SIMPLE (Semi-Implicit Method for Pressure Linked Equations) algorithm for the coupling of pressure and velocity, Patankar [19] and the line-by-line TDMA (Tridiagonal Matrix Algorithm) with block correction method for the solution of the systems of equations sequentially and iteratively.

The domain is divided into a uniform grid in such a way that the solid-fluid interface and the domain boundaries coincide with the faces of the control volumes. The harmonic mean is used to determine the diffusive coefficients at the interfaces of the control volume, Patankar [19]. The component velocities are allocated in a staggered grid. The criterion of convergence used is global convergence. This occurs when mass balance on each control volume and all domains are within a value of  $10^{-8}$  and the residuals

for  $u$ ,  $v$ ,  $T$  and  $p$  are about  $10^{-8}$ . Figure 3 shows the simplified flowchart of the home-built numerical code.

In order to achieve convergence and stability, a mesh study was performed for the two glass sheets of 8 mm thickness and 1m length, with the grids of 62x42, 88x50 and 120x80 volumes. The parameters taken as base for comparison are the fluid velocity  $v$  and the temperature, both at mid height of the channel. The variations of the temperature profile and velocity component at the center of double glass window were lower than 2% with volumes increasing from 88x50 to 120x80. Hence, the mesh of 88x50 volumes was adopted for the subsequent calculations of all considered cases. The total number of grid points across the window system subdivided as 11 grid points for each glass sheet and 30 grid points for the channel.

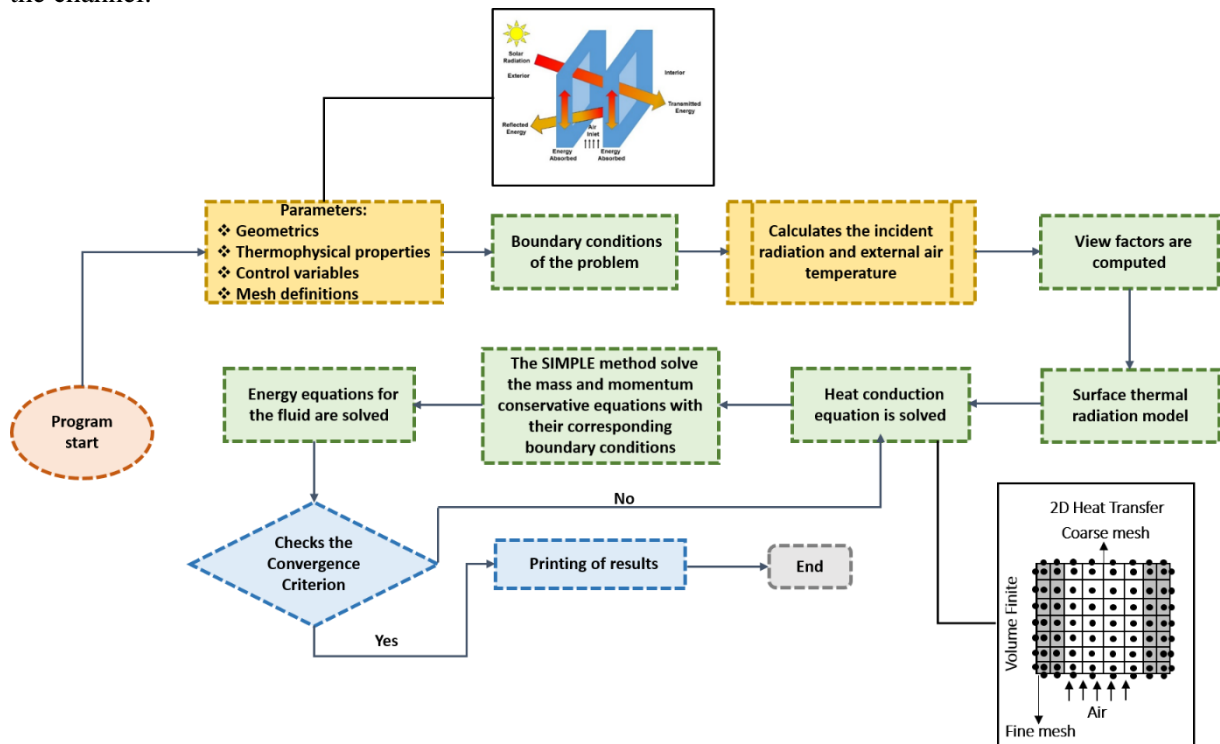


Figure 3. Simplified flowchart of the home-built numerical code.

## 4 Validation of the model

The FORTRAN home-built computational code was validated against available results in the literature. The first comparison was made with natural convection in laterally heated square cavity. Another comparison was made for natural convection between parallel vertical plates under constant temperature. The natural convection with surface radiation in a square cavity was also used for validation of the present code.

### 4.1 Comparison with the results of laterally heated square cavity

To validate the numerical code, the predicted average Nusselt number by the present code is compared with the values given by Davis [20], Frederick [21] and Palanigounder et al. [22] for different values of Rayleigh number as shown in Fig. 4. Figure 5 shows another comparison of Davis [20] temperature lines (isotherms) with isotherms found in the present study for different Rayleigh numbers. The agreement is good and confirms the adequacy and the accuracy of the present numerical method to study natural convection in a cavity with thermally active side walls.

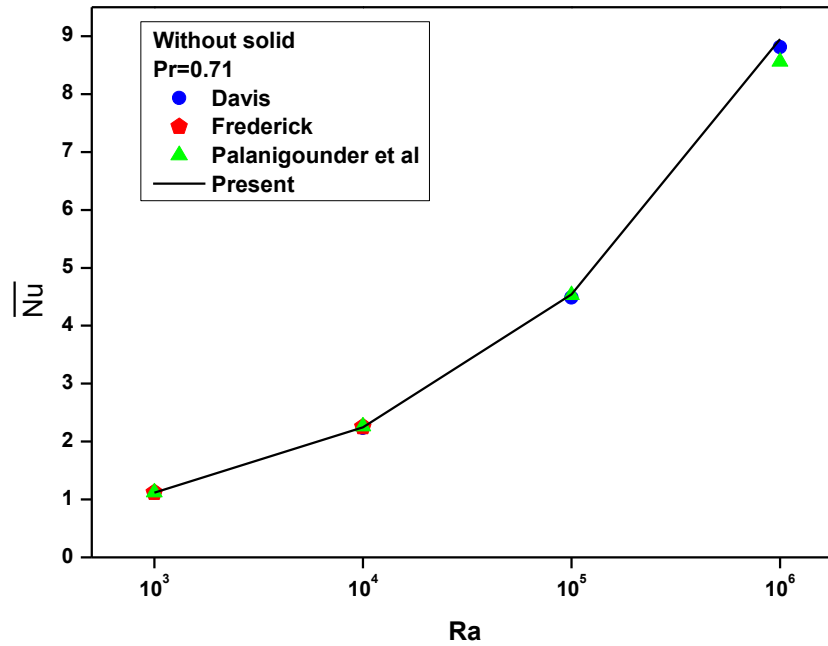


Figure 4. Variation of average Nusselt number with Rayleigh number for  $Pr = 0.71$ .

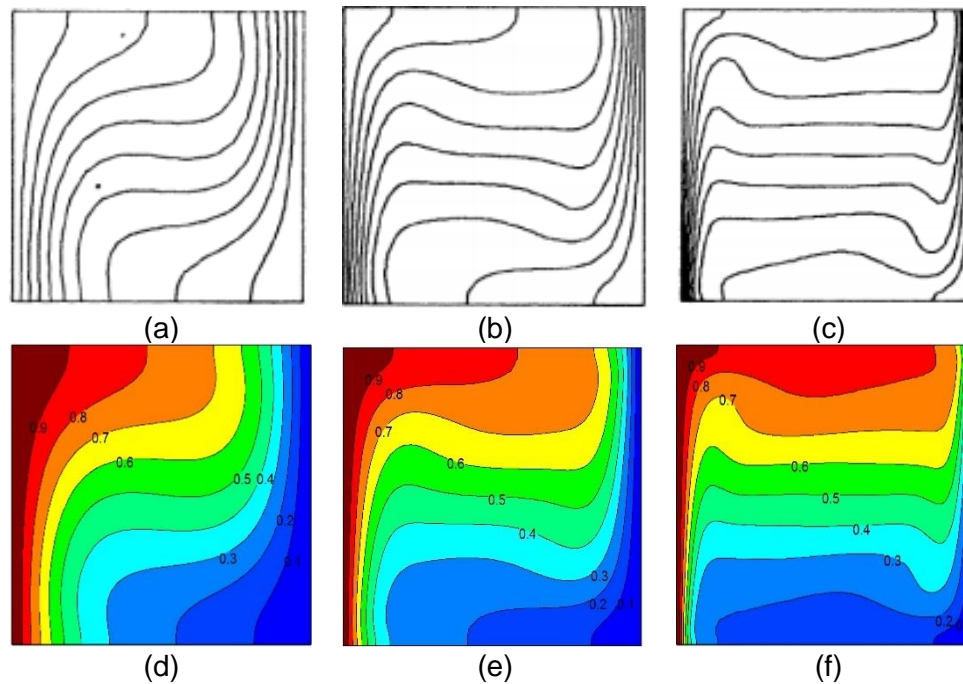


Figure 5. Comparison of isotherms within the cavity. (a) - (c) results from Vahl Davis [20] for  $Ra = 10^3, 10^4, 10^5$ . (d) - (f) results of the present study for  $Ra = 10^3, 10^4, 10^5$ .

#### 4.2 Comparison with the results of Natural convection between parallel vertical plates with symmetric heating under constant temperature

In this section a comparison is made with the natural convection problem between parallel vertical plates with symmetrical heating. Figure 6 shows the physical model of vertical plate flow used for numerical code verification.



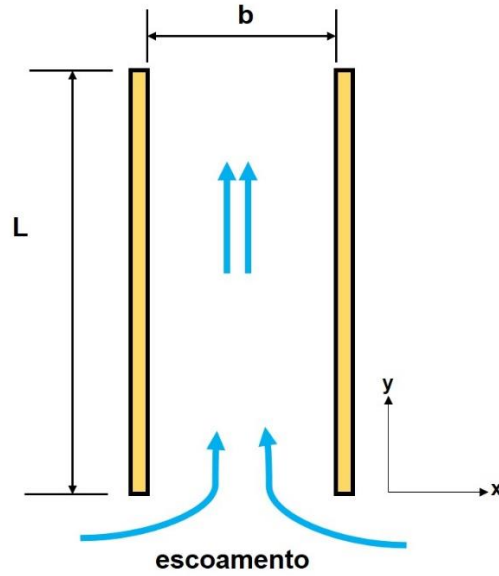


Figure 6. Symmetrical heating parallel vertical plates.

In order to generalize the numerical solution of the problem the following dimensionless variables are introduced:

$$X = \frac{x}{b} \quad Y = \frac{y}{b} \quad (20)$$

$$U = \frac{ub}{\alpha} \quad V = \frac{vb}{\alpha} \quad (21)$$

$$P = \frac{pb^2}{\rho\alpha^2} \quad (22)$$

$$\theta = \frac{T - T_o}{T_s - T_o} \quad (23)$$

$$Ra = \frac{g\beta(T_s - T_o)b^3}{\nu\alpha} \quad Ra^* = Ra \times \frac{b}{L} \quad (24)$$

$$Pr = \frac{\nu}{\alpha} \quad (25)$$

The results have been obtained for  $Pr=0.7$ , range of  $b/L$  (0.01 to 0.30) and  $Ra$  of (10 to  $10^8$ ). Comparison between the predicted average Nusselt number and the results developed by other investigators shows good agreement as in Fig. 7.

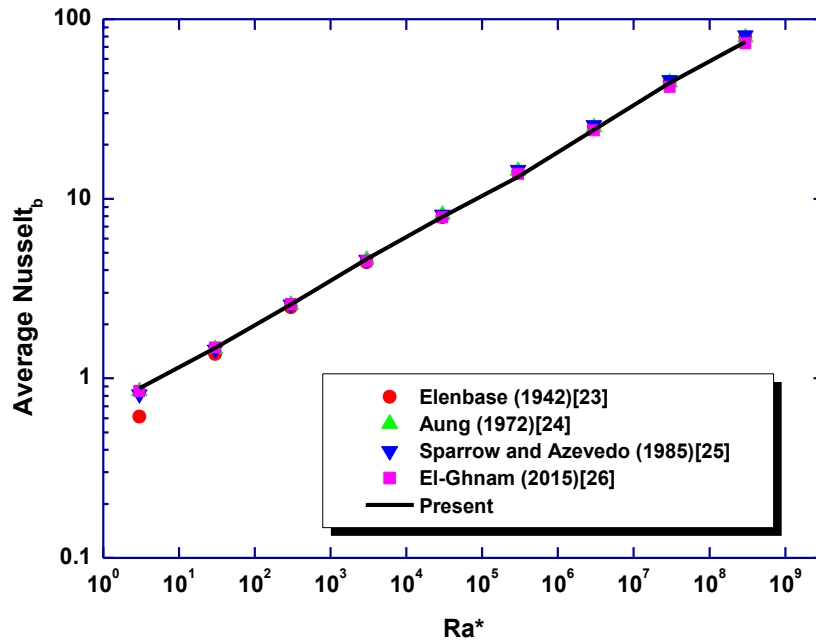
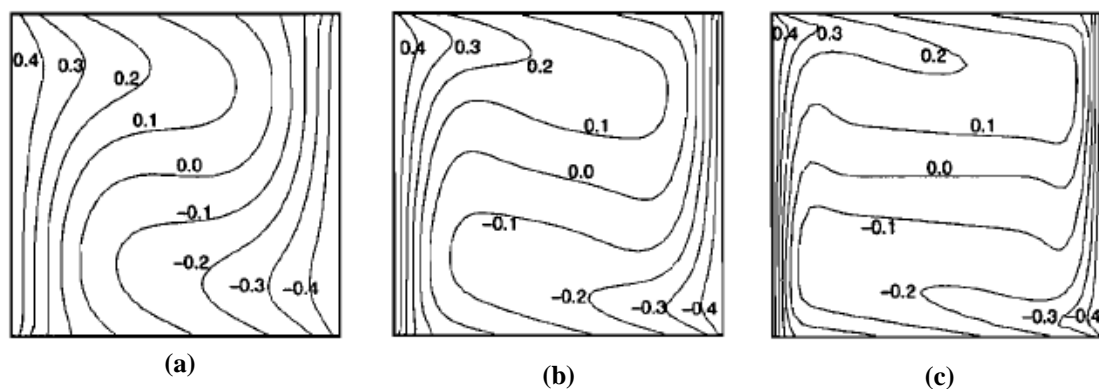


Figure 7. Symmetrical heating parallel vertical plates.

### 4.3 Natural convection with surface radiation in a square cavity

In order to verify the irradiative model, the results reported by Akiyama and Chong [27] for the conditions  $T_o=293.5$  K;  $Ra=(a)10^4, 10^5, 10^6$ ;  $\varepsilon=0.5$ ;  $\theta=29.35$  were reproduced in Fig. 8 which shows the comparisons of the isotherms. Surface radiation alters the distribution of the temperature on the insulated walls. The temperature rises at the bottom wall and decreases at the top wall, resulting in variations of the flow and temperature fields. The temperature gradients near the isothermal walls are relatively weakened, and the thermal boundary layers thicken by surface radiation. Symmetric contours of approximate center can also be observed because the smaller temperature difference between the two walls was generated in this place. It can be seen that good agreement is obtained in all the validation tests. Then, it can be concluded that the numerical code gives satisfactory results for the heat transfer problem.



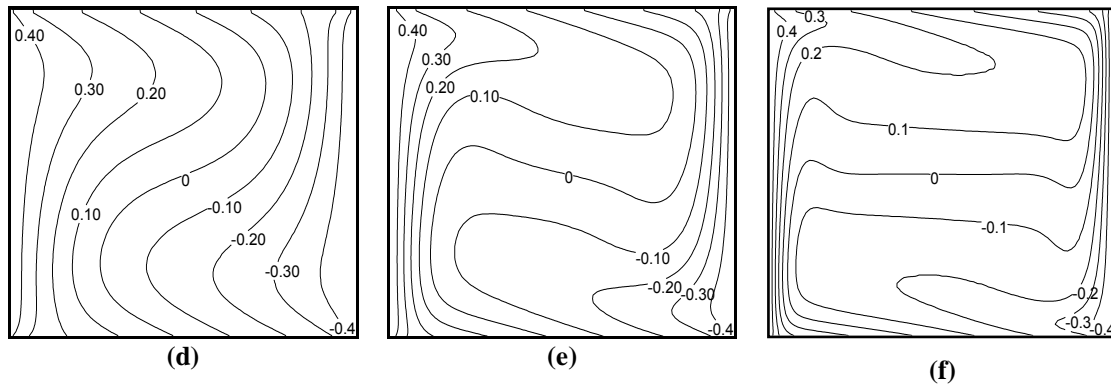


Figure 8. Effect of surface radiation on isotherms: (top a, b, c) from Akiyama and Chong [27] and (bottom d, e, f) predictions from the present study.

## 5 Results and discussion

The results of the present investigation in a ventilated double glass window system are shown and discussed below. The thickness of the glass plates was considered to be 8 mm and the temperatures of the indoor and outdoor environments are considered as 24°C and 36 °C, respectively. The temperature at the inlet of the channel will be equal to the temperature of the internal environment and the emissivities of the glass plates is equal to 0.84. The incident solar radiation is assumed to be 600 W/m<sup>2</sup>. The results presented below were obtained for permanent regime.

Figure 9 shows curves of the temperature profile of the fluid flowing through the ventilated window channel to the average channel height and obtained for different distance conditions between the glass plates (channel width). The distance between plates has been normalized in Fig. 10 to facilitate comparison of results. The distance between plates was varied from 0.5 cm to 5 cm. It can be observed that for distances of 5 cm only layers very close to the walls feel the effect of heating, whereas in the central region of the channel the fluid continues practically with the same inlet temperature (24°C). As the distance between plates decreases, the fluid layers closer to the centerline of the channel feel the effect of heating and the temperature profile has a shape that is closer to an inverted asymmetrical parabolic profile as in the case of plate distances smaller than 5 cm. For plate spacing of 0.5 and 1.0 cm the temperature profile is getting closer and closer to a linear profile, as in the case of pure diffusion. The reason for this is that for short distances between plates natural convection is compromised and the speed of induced flow will be small, making conduction heat transfer dominant in the process. This can be corroborated by the velocity curve  $v$  of the fluid in the channel, shown in Fig. 11.

In Fig. 11 it can be seen the behaviour of velocity  $v$  for the case where the distance between plates is 5 cm. In this case, it is observed that the velocity profile is almost uniform, presenting a higher velocity region near the left wall due to its higher temperature level in relation to the right wall. As the channel width decreases, the velocity profile  $v$  tends to be parabolic and symmetrical as if the plates were symmetrically heated. In fact, observing the temperature curves, we can verify that for the shortest distance between plates investigated the temperature difference is only 2° C. It is also observed in Fig. 11 that the magnitude of the velocity component  $v$  decreases as the distance between plates becomes smaller.

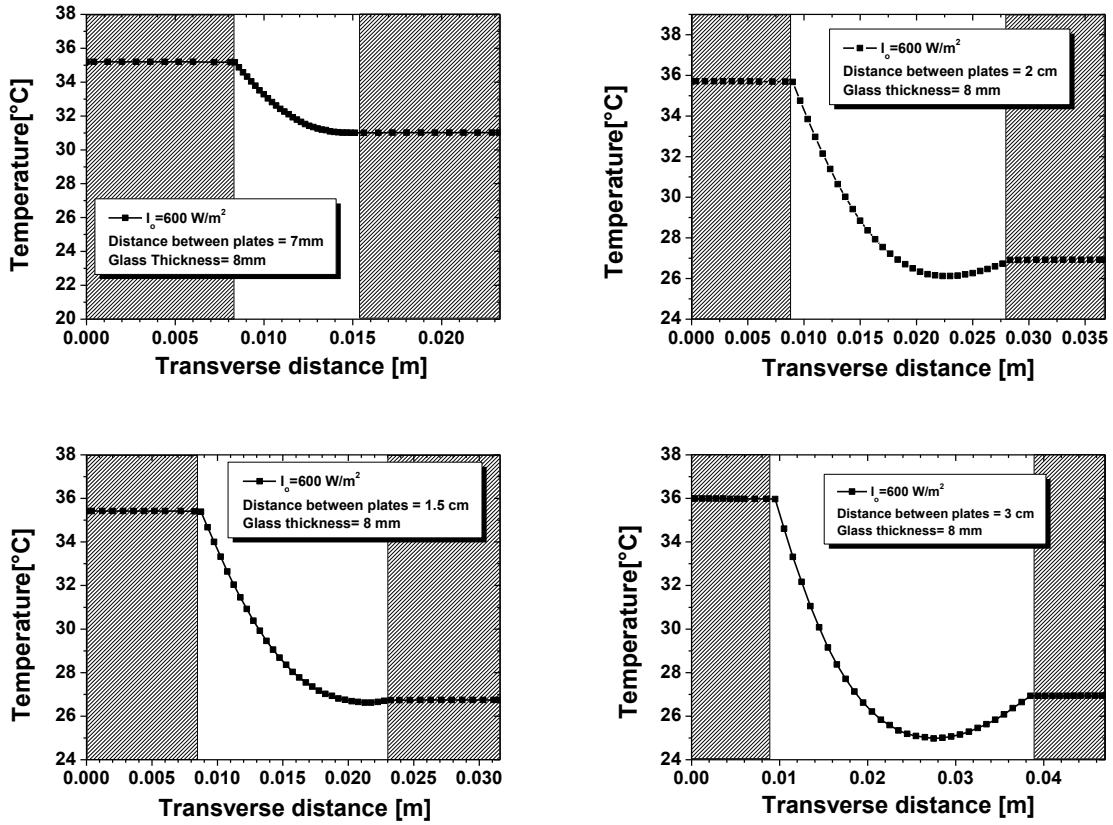


Figure 9. Temperature profiles.

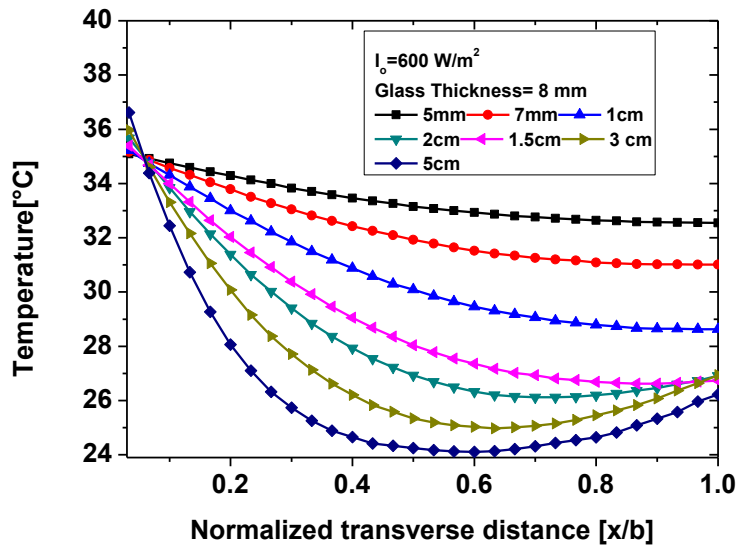


Figure 10. Comparison between temperature profiles at average window height as a function of normalized transverse distance.

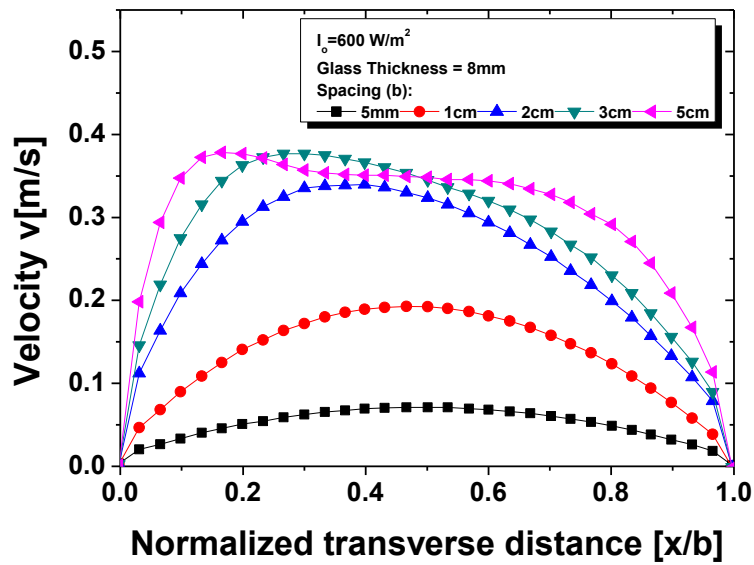


Figure 11. Comparison between the velocity profile  $v$  at the average window height as a function of the normalized transverse distance.

Figure 12 shows the variation of the percentage of heat gain as a function of the glass thickness for various spacing between the glass sheets of double glass window and for simple glass window. As can be verified the increase of thickness reduces the heat gain up to glass sheets spacing of about  $b \geq 0.025$  m, after which the heat gain reaches a steady state value. The reduction of the heat gain is more pronounced for the case of glass of thickness 8mm. For the case of simple glass window, as glass thickness increases, solar heat gain decreases.

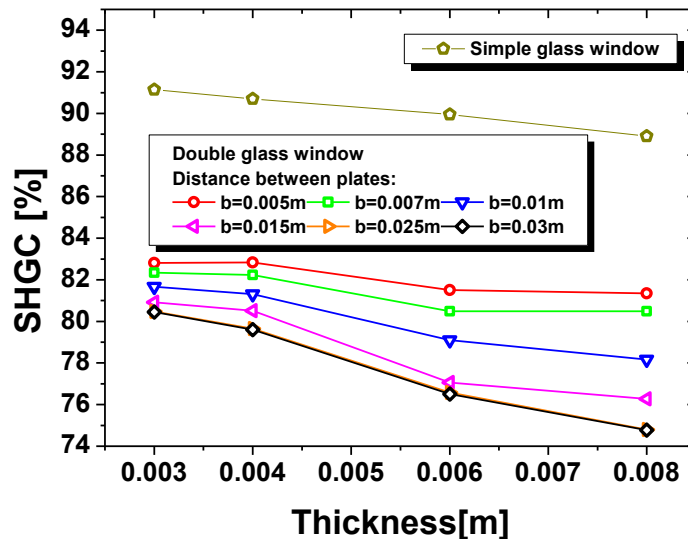


Figure 12. Variation of solar heat gain coefficient as a function of the glass thickness

## 6 Conclusions

A mathematical model developed to simulate fluid flow under natural convection conditions in a channel formed by parallel plates was presented here. It is verified that the computer program is able to determine in detail the velocity field and the temperature field of the fluid in the channel, and the distributions of these fields in the transverse direction of the channel can be presented at any position along the flow that generally is quite difficult to obtain experimentally. The code was used to simulate the thermal behaviour of a ventilated double glass window. The results show that for very close plate distances, natural convection is compromised and the fluid in the channel remains virtually stagnant, increasing the heat gain coefficient.

## Acknowledgements

The authors wish to thank the CNPq for the doctoral scholarship to the first author and wishes to thank the *Conselho Nacional de Desenvolvimento Científico e Tecnológico* (CNPq) for the PQ Research Grant 304372/2016-1 to the second author. The third author thanks the CAPES for the doctoral scholarship.

## References

- [1] S. Rheault and E. Bilgen. Heat Transfer analysis in an automated venetian blind window system. *Journal of Solar Energy Engineering*, vol. 111, pp. 89-85, 1989.
- [2] Z. Zhang, A. Bejan and J. Lage. Natural convection in a vertical enclosure with internal permeable screen. *Journal of Heat Transfer*, vol. 113, pp. 377-383, 1991.
- [3] H. Haddad and H. Elmahdy. Comparison of the monthly thermal performance of a conventional window and a supply-air window. *ASHRAE transactions*, vol. 104, pp. 1261-1270, 1998.
- [4] Y. Etzion and E. Erell. Controlling the transmission of radiant energy through Windows: a novel ventilated reversible glazing system. *Building and Environment*, vol. 35, pp. 433-444, 2000.
- [5] O. Aydin. Determination of optimum air-layer thickness in double pane windows. *Energy and Building*, vol. 32, pp. 303-308, 2000.
- [6] O. Aydin. Conjugate heat transfer analysis of double pane windows. *Building and Environment*, vol. 41, pp. 109-116, 2006.
- [7] K. Ismail and J. Henríquez. Modelling and simulation of a simple glass window. *Solar Energy Materials and Solar Cells*, vol. 80, pp. 355-374, 2003.
- [8] K. Ismail and J. Henríquez. Two-dimensional model for the double glass naturally ventilated window. *International Journal of Heat and Mass Transfer*, vol. 48, pp. 461-475, 2005.
- [9] K. Ismail and J. Henríquez. Simplified model for a ventilated glass window under forced air flow condition. *Applied Thermal Engineering*, vol. 26, pp. 295-302, 2006.
- [10] K. Ismail, C. Salinas and J. Henríquez. Comparison between PCM and glass windows and absorbing gas filled windows. *Energy and Buildings*, vol. 40, pp. 710-719, 2008.
- [11] K. Ismail, C. Salinas and J. Henríquez. A comparative study of naturally ventilated and gas filled windows for hot climates. *Energy Conversion and Management*, vol. 50, pp. 1691-1703, 2009.
- [12] T. Chow, Z. Lin, W. He, A. Chan and K. Fong. Use of ventilated solar screen window in warm climate. *Applied Thermal Engineering*, vol. 26, pp. 1910-1918, 2006.
- [13] T. Chow, Z. Lin, K. Fong, A. Chan and W. He. Thermal performance of natural airflow window in subtropical and temperate climate zones – a comparative study. *Energy Conversion and Management*, vol. 50, pp. 1884-1890, 2009.
- [14] T. Chow and Z. Lin. Innovative solar windows for cooling-demand climate. *Solar Energy Materials and Solar Cells*, vol. 94, pp. 212-220, 2010.
- [15] C. Gueymard and W. DuPont. Spectral effects on the transmittance, solar heat gain, and performance rating of glazing systems. *Solar Energy*, vol. 83, pp. 940-953, 2009.

- [16] J. Chávez-Galan and R. Almanza. Solar filters on iron oxides used as efficient windows for energy savings. *Solar Energy*, vol.81, pp. 13–19, 2009.
- [17] International Standard ISO 15099, Thermal Performance of Windows, Doors and Shadings Devices – Detailed Calculations, 2003.
- [18] R. Siegel, J. Howell and M. Pinar. *Thermal Radiation Heat Transfer*. CRC Press, New York, 2015
- [19] S. Patankar. *Numerical Heat Transfer and Fluid Flow*. Hemisphere, Washington, DC, 1980.
- [20] G. De Vahl Davis. Natural convection of air in a square cavity: a benchmark numerical solution. *International Journal of Numerical Methods in Fluids*, vol. 3, pp. 249–264, 1983.
- [21] L. Frederick. Natural convection in an inclined square enclosure with a partition attached to its cold wall. *International Journal Heat Mass Transfer*, vol. 32, pp. 87, 1989
- [22] K. Palanigounder, N. Nithyadevi and N. Chiu-On. Natural convection in enclosures with partially thermally active side walls containing internal heat sources. *Physics of Fluids*, vol. 20, pp. 097-104, 2008.
- [23] W. Elenbaas. Heat dissipation of parallel plates by free convection. *Physics*, vol.9 (1942) pp.1-28.
- [24] W. Aung, S. Fletcher and V., Sernas. Developing laminar free convection between flat plates with asymmetric heating. *International Journal Heat Mass Transfer*, vol.15, pp. 2293-2308, 1972.
- [25] E. Sparrow and L. Azevedo. Natural convection in open-ended inclined channels. *Journal of Heat Transfer*, vol. 107, pp. 893-901, 1985.
- [26] R. El-Ghnam. Numerical Investigation of Natural Convection Heat Transfer between Two Vertical Plates with Symmetric Heating. *International Journal of Thermal Technologies*, vol. 5, pp. 31-44, 2015.
- [27] M. Akiyama and Q. P. Chong. Numerical analysis of natural convection with surface radiation in a square enclosure. *Numerical Heat Transfer, Part A: Applications*, vol. 32(4), pp. 419–433, 1997.

## Nomenclature

$b$	width of channel (m)
$b/L$	width-to-length ratio
$cp$	specific heat ( $\text{J kg}^{-1} \text{K}^{-1}$ )
$g$	gravitational acceleration ( $9.81\text{ms}^{-2}$ )
$h$	convective heat transfer coefficient ( $\text{W/m}^2\text{K}$ )
$H$	height of the glass (m)
$I_o$	incident solar radiation ( $\text{W/m}^2$ )
$k$	thermal conductivity ( $\text{W/mK}$ )
$L$	channel length (m)
$Nu$	local Nusselt number ( $hb/k$ )
$\overline{Nu}$	average Nusselt number ( $\overline{hb/k}$ )
$p$	pressure ( $\text{N/m}^2$ )
$P$	dimensionless pressure ( $pb^2/\rho\alpha^2$ )
$Pr$	Prandtl number ( $\nu/\alpha$ )
$q$	heat flux ( $\text{W/m}^2$ )
$Ra$	Rayleigh number ( $g\beta(T_s-T_o)b^3/\nu\alpha$ )
$Ra^*$	modified Rayleigh number ( $Ra \times b/L$ )
$SHGC$	solar heat gain coefficient
$t$	glass thickness (m)
$T$	temperature (K)
$T_g$	glass temperature (K)
$T_o$	ambient temperature (K)
$T_s$	wall temperature (K)
$u$	velocity components in the x direction (m/s)
$U$	dimensionless velocity components in the x direction ( $ub/\alpha$ )
$v$	velocity components in the y direction(m/s)
$V$	dimensionless velocity components in the y direction ( $vb/\alpha$ )

$x$	horizontal cartesian coordinates (m)
$X$	dimensionless Cartesian coordinate (x/b)
$y$	vertical Cartesian coordinates (m)
$Y$	dimensionless Cartesian coordinate (y/b)

*Greek symbols*

$\alpha$	thermal diffusivity (m <sup>2</sup> /s)
$\alpha_g$	absorptance of clear glass
$\beta$	thermal expansion coefficient (K <sup>-1</sup> )
$\theta$	dimensionless temperature (T-T <sub>o</sub> /T <sub>s</sub> -T <sub>o</sub> )
$\kappa$	extinction coefficient (m <sup>-1</sup> )
$\mu$	dynamic viscosity (kgm <sup>-1</sup> s <sup>-1</sup> )
$\rho$	density (kg m <sup>-3</sup> )
$\nu$	kinematic viscosity (m <sup>2</sup> /s)

*Subscripts*

<i>cond</i>	conduction heat transfer
<i>conv</i>	convection heat transfer
<i>ext</i>	external ambient
<i>g</i>	glass
<i>int</i>	internal ambient
<i>rad</i>	radiation heat transfer
1,2	glass number